.

Article DOI: 10.18500/0869-6632-003009

Spectrum of exchange spin waves in a one-dimensional magnonic crystal with antiferromagnetic ordering

V. D. Poimanov

Enikolopov Institute of Synthetic Polymeric Materials
of Russian Academy of Sciences, Moscow, Russia
Moscow State University of Geodesy and Cartography, Russia
E-mail: Vladislav.Poymanow@yandex.ru

Received 21.04.2022, accepted 21.07.2022, published 30.09.2022

Abstract. *Purpose* of the study is to show that the conditions for the propagation of exchanged spin waves (ESWs) in an asymmetric superlattice with antiferromagnetically ordered cells depend significantly on the chirality of the precession of the ESW magnetization (polarization, "magnon pseudospin"). *Method.* When constructing the EWS spectra, the Croning–Penny model (transfer-matrix method) and the Landau–Lifshitz equation are used to determine the nature of the waves in the cells. In the case of a uniaxial medium, there is only one type of ESW, therefore, when fields are joined at the boundary, the conservation of chirality is an essential factor due to which the ESW in one cell is always traveling, and in the other — evanescent. Thus, a superlattice for ESW is an effective periodic "potential" in which asymmetry can be realized either by applying an external field, or by a difference in the thickness and/or physical properties of the cell materials. *Results.* Based on the analysis of the spectrum, maps of the transmission zones for ESW of different chirality were constructed in three representations — "Bloch wave number – frequency", "frequency – relative cell thickness", as well as in the plane of cell wave numbers. It is shown that the presence of asymmetry leads to a difference in the width of the transmission zones for waves of different chirality. For a finite structure, the frequency dependences of the transmission and reflection coefficients of the ESW are plotted. An increase in the attenuation of the ESW near the boundaries of the transmission zones was also found. *Conclusion.* The results of the study can be used in the design of magnon valves and other devices based on ESW, in which their chirality can be controlled.

Keywords: magnetic superlattice (crystal), exchanged spin waves, transmission bands, precession chirality, scattering coefficients.

Acknowledgements. The author would like to thank V. V. Kruglyak (University of Exeter) for fruitful discussions and recommendations.

For citation: Poimanov VD. Spectrum of exchange spin waves in a one-dimensional magnonic crystal with antiferromagnetic ordering. Izvestiya VUZ. Applied Nonlinear Dynamics. 2022;30(5):644–652. DOI: 10.18500/0869-6632-003009

Introduction

The fundamental basis for the operation of any logical device is the ability to differentiate at least two of its states. For example, in electronics, the logical "zero"and "one"are identified with the absence and presence of current. In quantum physics, the states of two electrons with the same spatial wave function may differ in the spin value and their behavior in a zero magnetic field will be the same. The external magnetic field allows you to select their spin number, as a result of which their energies will be different.

The presence of properties specific to signal transmission in exchange spin waves (ESW) opens up a wider range of possibilities for their control [1]. Such a parameter for spin waves is their polarization (chirality of the precession of magnetization). By analogy with the model mentioned above, a certain chirality of the ESW can be identified with «magnon pseudospin».

In the simplest case of an isolated magnetic moment, the nature of its motion is a Larmor precession, in which the end of the magnetization vector describes a circle in the clockwise direction when observed along the equilibrium magnetization (the so-called right-hand precession). Under the same conditions, precession in the opposite direction is anti-harmonic and, by virtue of the Landau equation−Lifshitz, is impossible for an isolated magnetic moment. However, if there is an exchange field described by the multiplier $\lambda^2 k^2$ (λ — exchange length, k — wave number), the effective field is negative if the wave number is imaginary. The corresponding wave, called evanescent (attenuating), is localized near the boundary and cannot exist in an unlimited medium [2–7]. Note that evanescent waves in magnets are quite common. However, they are magnetostatic and inhomogeneous along the thickness of the film [8]. In this work, the inhomogeneous ESW is localized near the boundary and attenuates along the film itself.

ESW scattering and boundary conditions for them were considered earlier [9, 10]. In the works [2–4] it was shown that in a magnetic structure with uniaxial anisotropy, traveling and evanescent ESW have mutually opposite circular polarizations with respect to equilibrium magnetization. When crossing the boundary of cells with opposite magnetization, the traveling wave becomes evanescent and vice versa. In this case, polarization (pseudospin) ESW is saved [2]. Using this circumstance, we consider its propagation in a one-dimensional magnon crystal with cells in which the equilibrium magnetizations are oriented antiparallel. We investigate the transformation of the transmission spectrum of such a structure, due to both the difference in cell thicknesses and the application of an external field.

1. ESW propagation in an unlimited antiferromagnetic superlattice

Let's choose the normal to the boundaries of the layers as the z axis, and the direction of the light axis of uniaxial anisotropy and equilibrium magnetization of the cells — as the x axis, with respect to which we will determine the polarization of the ESW. In a uniaxial medium in each of the cells, the ESW are either traveling or evanescent, depending on the relationship between the polarization of the wave and the orientation of the equilibrium magnetization [3], for which the indices "U"and "D"denote a parallel or antiparallel orientation with respect to the x axis, respectively.

Note that both types of waves can be present in biaxial materials [4].

The structure in Fig. 1 by wave properties is a well-known Croning-Penny model. However, the difference in the geometric or magnetic parameters of the cells leads to a difference in the conditions of the propagation of ESW with different polarizations. A similar effect is achieved by applying an external field. As a result, the transmission spectrum may have a non-reciprocal character. In a symmetrical structure, for which the external field is zero and the cell thicknesses are the same, there are no non-reciprocity effects. That is, when the sign of the equilibrium magnetizations in the cells changes, the spectrum does not change its appearance.

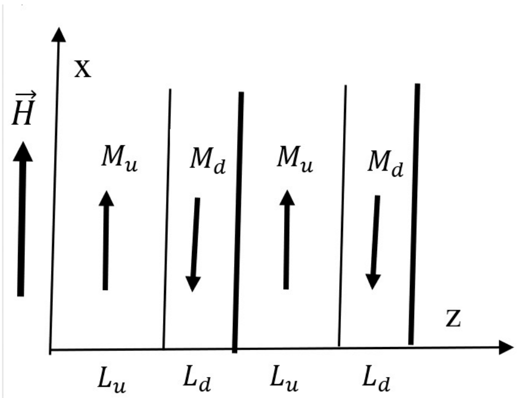

Fig. 1. The geometry of the structure. Cell U occupies an area $z = [0,\ L_u] + NL$ $(L = L_u + L_d)$, and cell D occupies an area $z = [L_u,\ L] + NL$, where N — is integer

In uniaxial materials, where precession is circular, the magnetization dynamics can be set by a single scalar variable ψ, which is the amplitude of the normalized dynamic magnetization [10]. Using the standard method of the transfer matrix [11], we find that the values of dynamic variables through the period are related by the relation:

$$\begin{pmatrix} \psi \\ \psi' \end{pmatrix}(z+L) = \hat{T}, \quad \begin{pmatrix} \psi \\ \psi' \end{pmatrix}(z) = e^{iKL}\begin{pmatrix} \psi \\ \psi' \end{pmatrix}(z), \tag{1}$$

where "stroke"means the derivative of the coordinate along the normal to the boundary,

$$\hat{T} = \begin{pmatrix} \cos(k_d L_d) & \dfrac{\sin(k_d L_d)}{k_d} \\ -k_d \sin(k_d L_d) & \cos(k_d L_d) \end{pmatrix} \begin{pmatrix} \cos(k_u L_u) & \dfrac{\sin(k_u L_u)}{k_u} \\ -k_u \sin(k_u L_u) & \cos(k_u L_u) \end{pmatrix}, \tag{2}$$

K — the Bloch wave number. The following dispersion equation has the form:

$$\cos KL = \cos(k_u L_u)\cos(k_d L_d) - \frac{1}{2}\left(\frac{k_u}{k_d} + \frac{k_d}{k_u}\right)\sin(k_u L_u)\sin(k_d L_d), \tag{3}$$

where k_u,k_d are the wave numbers in the corresponding cells, which are from the Landau–Lifshitz equation:

$$\dot{\mathbf{M}}_n + \gamma[\mathbf{M}_n \times \mathbf{H}_{\text{ef}}] = 0. \tag{4}$$

Taking into account the type of effective field

$$\mathbf{H}_{\text{ef},n} = H\mathbf{n}_x - (\lambda_n^2 k^2 + \beta_n)(m_{ny}\mathbf{n}_y + m_{nz}\mathbf{n}_z), \tag{5}$$

where λ_n — the exchange length, β_n — the constant of light-axial anisotropy, $\mathbf{H} > 0$ — the magnitude of the external field, and the periodic dependence of dynamic variables $\mathbf{m}_n \exp i(k_n z - \omega t) = (0, m_{ny}, m_{nz})$ from (4) we obtain linearized equations for the cyclic components of each layer ($m_{n\pm}$ = $= m_y \pm i m_z$):

$$\left(\lambda_n^2 k^2 + \beta_n + \sigma_n \frac{\omega_H \pm \omega}{\omega_n}\right) m_{n\pm} = 0, \tag{6}$$

where $\omega_H = \gamma H$, $\sigma_n = \pm 1$ — markers of the orientation of the equilibrium magnetization with respect to the axis x.

Note that traveling waves with Larmor precession in an unbounded structure have right polarization in U-cells and left — in D-cells. On the contrary, the right waves in D-cells and the left — in U-cells are evanescent (with an anti-Larmor precession)..

When the right wave (R) propagates, in which the rotation of the magnetization occurs clockwise when observed along the x axis, the component $_{n-}$ is nonzero. The equation (6) for it has the form:

$$\left(\lambda_n^2 k_n^2 + \beta_n + \sigma_n \frac{\omega_H - \omega}{\omega_n}\right) m_{n-} = 0. \tag{7}$$

Then in this case

$$k_{uR}^2 = \frac{\omega - (\beta_u \omega_u + \omega_H)}{\omega_u \lambda_u^2} > 0, \quad k_{dR}^2 = -\frac{\omega + (\beta_d \omega_d - \omega_H)}{\omega_d \lambda_d^2} < 0, \tag{8}$$

that is, — in the U-cell the wave is traveling, and in the D-cell — evanescent. In this case, the conditions must be met for the frequency $\omega > \omega_0 = \beta_u \omega_u + \omega_H$ and the value of the external field

$\beta_d\omega_d - \omega_H > 0$. The first of them means that the frequency of the propagating ESW is higher than the activation one (the frequency of homogeneous ferromagnetic resonance in the U-cell), and the second ensures the stability of the antiparallel orientation of the magnetization with respect to the field in the D-cell.

For the left wave (L), where the rotation of the magnetization occurs counterclockwise when observed along the axis x, $m_{n+} \neq 0$:

$$\left(\lambda_n^2 k_n^2 + \beta_n + \sigma_n \frac{\omega_H + \omega}{\omega_n}\right) m_{n+} = 0. \qquad (9)$$

In this case we get

$$k_{uL}^2 = -\frac{\omega + (\beta_u\omega_u + \omega_H)}{\omega_u\lambda_u^2} < 0, \quad k_{dL}^2 = \frac{\omega - (\beta_d\omega_d - \omega_H)}{\omega_d\lambda_d^2} > 0. \qquad (10)$$

When switching the equilibrium magnetization, the type of waves in each cell also changes. The wave numbers of traveling and evanescent waves for any frequency are related by the relation

$$\omega_u\lambda_u^2 k_u^2 + \omega_d\lambda_d^2 k_d^2 = -\left(\beta_u\omega_u + \beta_d\omega_d\right), \qquad (11)$$

where frequency is not included. By analogy with [12, 13], let's call the equation (11) a spectrum line.

Let's consider the most important special case when the magnetic parameters of the layers are the same, and introduce dimensionless variables — wave numbers $\xi_u = k_u^2 L^2$, $\xi_d = k_d^2 L^2$, the relative thickness of the layers $L_u/L = \varepsilon$, $L_d/L = 1 - \varepsilon$ and the parameter $\Delta = L^2/\lambda^2$. Then (3) and (11) will correspond in form:

$$\cos KL = \cos\left(\sqrt{\xi_u}\varepsilon\right)\cos\left(\sqrt{\xi_d}\,(1-\varepsilon)\right) + \beta\Delta\frac{\sin\left(\sqrt{\xi_u}\varepsilon\right)}{\sqrt{\xi_u}}\frac{\sin\left(\sqrt{\xi_d}\,(1-\varepsilon)\right)}{\sqrt{\xi_d}}, \qquad (12)$$

$\xi_u + \xi_d = -2\beta\Delta$.

The reduced spectrum has symmetry with respect to the replacement of $U \leftrightarrow$D (which corresponds to the switching of equilibrium magnetizations) and the simultaneous replacement of $\varepsilon \leftrightarrow (1-\varepsilon)$, since such a replacement corresponds to the transition to the same structure shifted by a cell. Simultaneously with the switching of magnetizations, the type of waves (traveling $\leftrightarrow$ evanescent) in each cell changes for both types of polarization. Dimensionless wave numbers have the form:

$$\xi_{uR} = \Delta\,(\Omega - \beta - \Omega_H), \quad \xi_{dR} = -\Delta\,(\Omega + \beta - \Omega_H) \qquad (13)$$

for the right wave and

$$\xi_{uL} = -\Delta\,(\Omega + \beta + \Omega_H), \quad \xi_{dL} = \Delta\,(\Omega + \beta + \Omega_H) \qquad (14)$$

for the left. Here $\Omega = \omega/\omega_M$, $\Omega_H = \omega_H/\omega_M$ — dimensionless frequencies. As can be seen from (12), the transformation of the transmission zones (ZT) is reduced simply to a frequency shift.If the external magnetic field is positive — the ZT of the right waves shift up, and the ZT of the left waves shift down, and vice versa.For both types of polarization, the number of ZT waves of both polarizations is unlimited for any ε. However, their width decreases rapidly with the growth of the zone number.

On fig. 2 shows the scheme of the ZT in the diagram «relative layer thickness U—dimensionless frequency of the ESW Ω» for each type of polarization. The ZT correspond

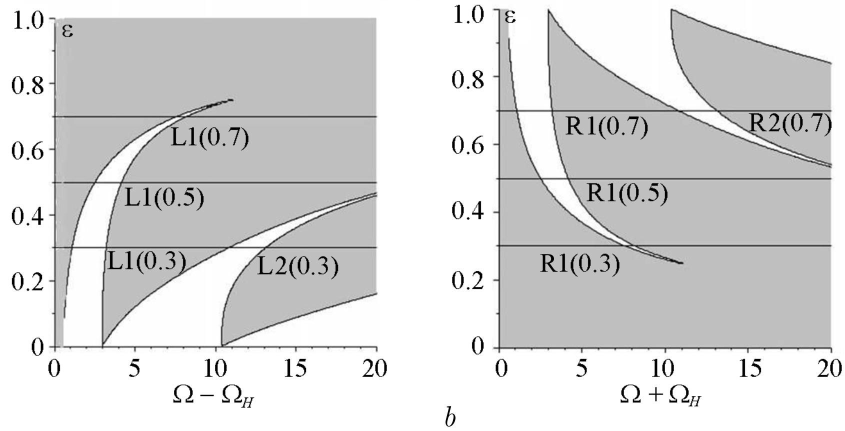

a *b*

Fig. 2. The map of the transmission zones of the left (a) and right (b) waves on the diagram of parameters "relative layer thickness U — dimensionless frequency of ESW Ω"

to the intersection of horizontal lines $\varepsilon = 0.1$, 0.3, 0.5, 0.7 and 0.9 with light areas. For all values except $\varepsilon = 0.5$, the forbidden zone schemes for right and left waves differ, which clearly illustrates the difference in propagation conditions due to their polarization.

For each of these values, ε in Fig. 3 the zone map is shown in a different representation — in the variables $k_u^2\lambda^2, k_d^2\lambda^2$, where the ZT corresponds to the intersection of the light regions with the spectrum line. The right waves correspond to the zones in the fourth quarter, and the left— in the second. In Fig. 4 ZT are constructed in variables «Bloch wave number — dimensionless frequency Ω». Frequency dependences for the right waves, the external positive field shifts up, and for the left — down.

Thus, presented in Fig. 2, 3, 4 ZT illustrate the dependence of the conditions for the propagation of ESW on their polarization when the symmetry of the structure in the cell is violated. With an increase in ε, ZT right waves increase and thicken, and the left— vice versa. This is due to a decrease in the relative volume of cells in which the waves are evanescent. The obtained dependences are symmetric with respect to the simultaneous replacement of the polarization $L \leftrightarrow$ R and the relative thickness of $\varepsilon \leftrightarrow 1 - \varepsilon$.

Taking into account the Hilbert attenuation leads to the appearance of imaginary terms in

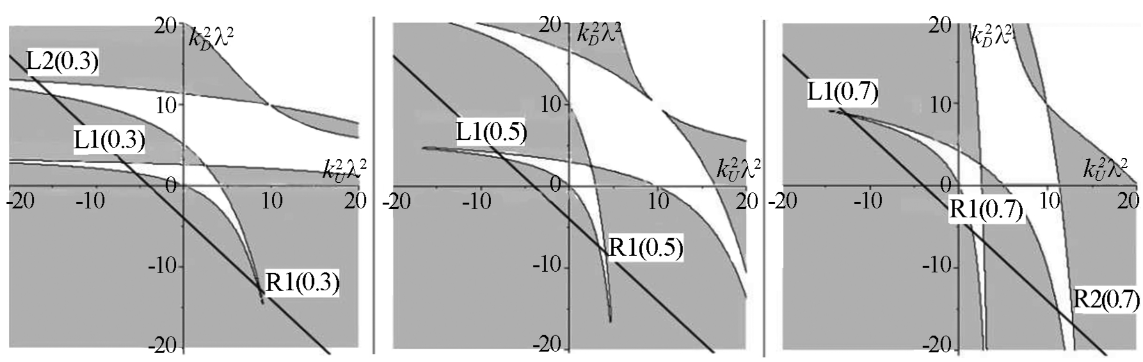

Fig. 3. Maps of allowed (white background) and forbidden (gray) zones for relative layer thicknesses U at $\varepsilon = 0.3$, 0.5 and 0.7, built on the diagram of variables $\left(k_u^2\lambda^2, k_d^2\lambda^2\right)$. The straight line depicts the spectrum line (8)

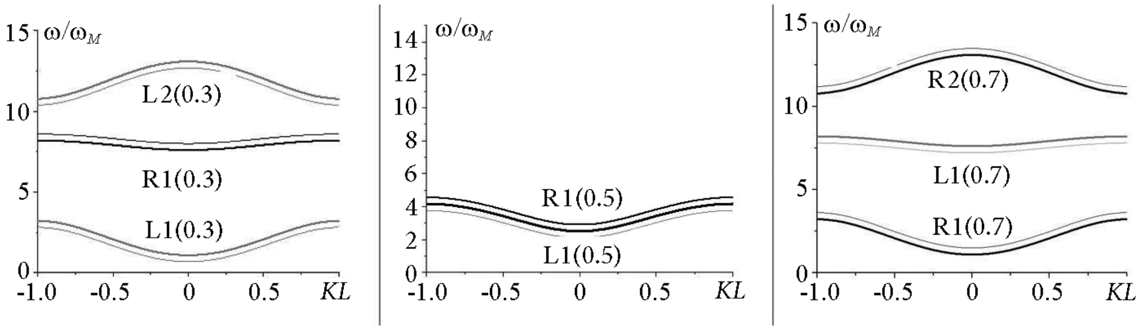

Fig. 4. Dependences of the dimensionless frequency on the Bloch wave number for $\varepsilon = 0.3$, 0.5 and 0.7. Black lines correspond to the right waves, gray lines to the left. Thick lines correspond to $\Omega_H = 0$, thin lines — $\Omega_H = 0.4$

expressions for wave numbers:

$$\lambda_U^2 k_{RU}^2 = \frac{\omega\,(1 + i\alpha_U) - \omega_H}{\omega_U} - \beta_U, \quad \lambda_D^2 k_{RD}^2 = -\frac{\omega\,(1 - i\alpha_D) - \omega_H}{\omega_D} - \beta_D, \tag{15}$$

$$\lambda_U^2 k_{LU}^2 = -\frac{\omega\,(1 - i\alpha_U) + \omega_H}{\omega_U} - \beta_U, \quad \lambda_D^2 k_{LD}^2 = \frac{\omega\,(1 + i\alpha_D) + \omega_H}{\omega_D} - \beta_D, \tag{16}$$

where α_U, α_D are the Hilbert decay constants in U and in D cells, respectively.

In Fig. 5 for the case of ε=0.7, the frequency dependence of the imaginary part of the Bloch wave number inversely proportional to the depth of propagation of the ESW in the superlattice is shown. With increasing frequency (and zone number), absorption increases.

From Fig. 5 it can be seen that this propagation depth is determined by the value of the Hilbert constant in the cell in which the wave is traveling for this type of polarization and weakly depends on the attenuation value in the cell where this wave is evanescent, since the imaginary part in it is a small additive. There is an increase in this absorption at the edges of the ZT. This behavior of the transmission propagation depth can be explained by a decrease in the group velocity at the boundaries of the zones. This allows us to draw an analogy between the described phenomenon caused by the spatial distribution of the amplitude inside the cells and the well-known Bormann effect [14–16]. The effect of the latter on the attenuation gain is discussed in more detail in [17].

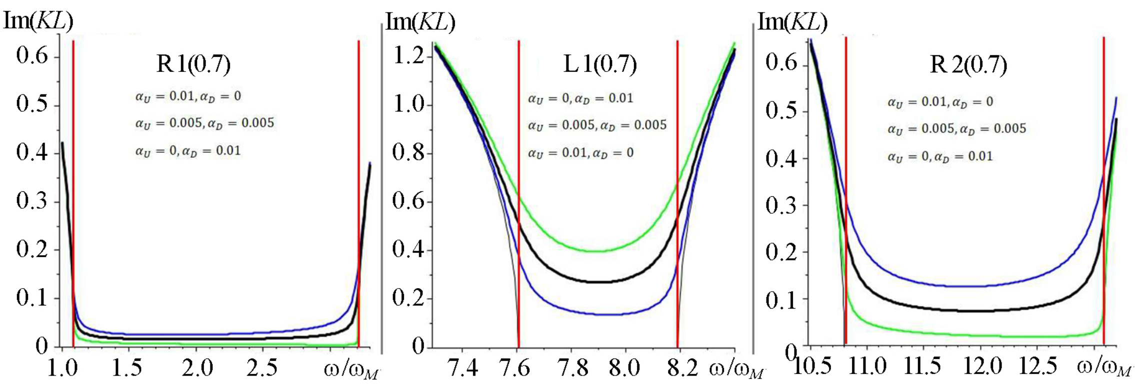

Fig. 5. Frequency dependence of the imaginary part of the Bloch wave number for the values of the relative thickness and Hilbert parameters indicated on the graphs. The vertical red lines correspond to the boundaries of the pass zones. The blue line corresponds to the values of the Hilbert damping parameters $\alpha_U = 0.01$, $\alpha_D = 0$, black — $\alpha_U = \alpha_D = 0.05$, green — $\alpha_U = 0$, $\alpha_D = 0.01$ (color online)

2. Scattering by a superlattice with a finite number of layers

Consider an unbounded homogeneous magnetic structure in which the equilibrium magnetization is oriented antiparallel to the x axis. The traveling waves in it are waves with left-hand polarization. Let N plane defects with a thickness of d_U be embedded in such a structure in the form of layers of the same material with an equilibrium magnetization parallel to the x axis at a distance of d_D between each other. Let's write the traveling wave field to the left of the superlattice in the form:

$$\psi_0(z) = e^{ik_{LD}z} + Re^{-ik_{LD}z}, \quad \psi_0'(z) = ik_{LD}\left(e^{ik_{LD}z} - Re^{-ik_{LD}z}\right), \tag{17}$$

where k_{LD} is the wave number of the incident wave of left-hand polarization to the left of the structure,
R is the amplitude reflection coefficient.

Due to continuity conditions

$$\begin{pmatrix}\psi_\downarrow \\ \psi_\downarrow'\end{pmatrix}(0+0) = -\begin{pmatrix}\psi_0 \\ \psi_0'\end{pmatrix}(0-0) = -\begin{pmatrix}1 & 1 \\ ik_{LD} & -ik_{LD}\end{pmatrix}\begin{pmatrix}1 \\ R\end{pmatrix}. \tag{18}$$

The index in the form of an arrow indicates the direction of equilibrium magnetization in this cell. Similarly, the field to the right of the structure:

$$\psi_f(z) = Te^{ik_{LD}(z-(N-1)d-d_D)}, \quad \psi_f'(z) = ik_{LD}Te^{ik_{LD}(z-(N-1)d-d_D)}, \tag{19}$$

where T is the amplitude coefficient of passage.

The system of boundary conditions for $z = d$ has the form:

$$\begin{pmatrix}\psi_f \\ \psi_f'\end{pmatrix}(d+0) = -\begin{pmatrix}\psi_\uparrow \\ \psi_\uparrow'\end{pmatrix}(d-0) = \begin{pmatrix}T \\ ik_{LD}T\end{pmatrix}. \tag{20}$$

Thus, the scattering coefficients satisfy the system:

$$\begin{pmatrix}T \\ ik_{LD}T\end{pmatrix} = \hat{T}_N\begin{pmatrix}1 & 1 \\ ik_{LD} & -ik_{LD}\end{pmatrix}\begin{pmatrix}1 \\ R\end{pmatrix} = \begin{pmatrix}T_{11} & T_{12} \\ T_{21} & T_{22}\end{pmatrix}\begin{pmatrix}1+R \\ ik_{LD}(1-R)\end{pmatrix}, \tag{21}$$

where $\hat{T}_N = \hat{T}_e(d_U)\left(\hat{T}_p(d_D)\hat{T}_e(d_U)\right)^{N-1}$. From here

$$R = \frac{(k_pT_{N22} - iT_{N21}) - \left(k_pT_{N11} + ik_p^2T_{N12}\right)}{(k_pT_{N22} + iT_{N21}) + \left(k_pT_{N11} - ik_p^2T_{N12}\right)}, \tag{22}$$

$$T = \frac{2i\left(k_p^2T_{N22}T_{N12} + T_{N21}T_{N11}\right)}{(k_pT_{N22} + iT_{N21}) + \left(k_pT_{N11} - ik_p^2T_{N12}\right)}. \tag{23}$$

In Fig. 6 the frequency dependence of the reflection and transmission coefficients of the ESW left polarization axis for a structure of 10 antiferromagnetic layers is presented.

Comparison of Fig. 6 for the left wave at $\varepsilon = 0.3$, 0.5 and 0.7 shows the dependence of the scattering efficiency on the relative thickness in the transmission zones. The observed peaks are caused by interference of waves reflected from the cell boundaries and are most pronounced in the first zone. For $\varepsilon = 0.7$, when the volume of "allowed"cells for the left wave is relatively small and scattering is weaker.

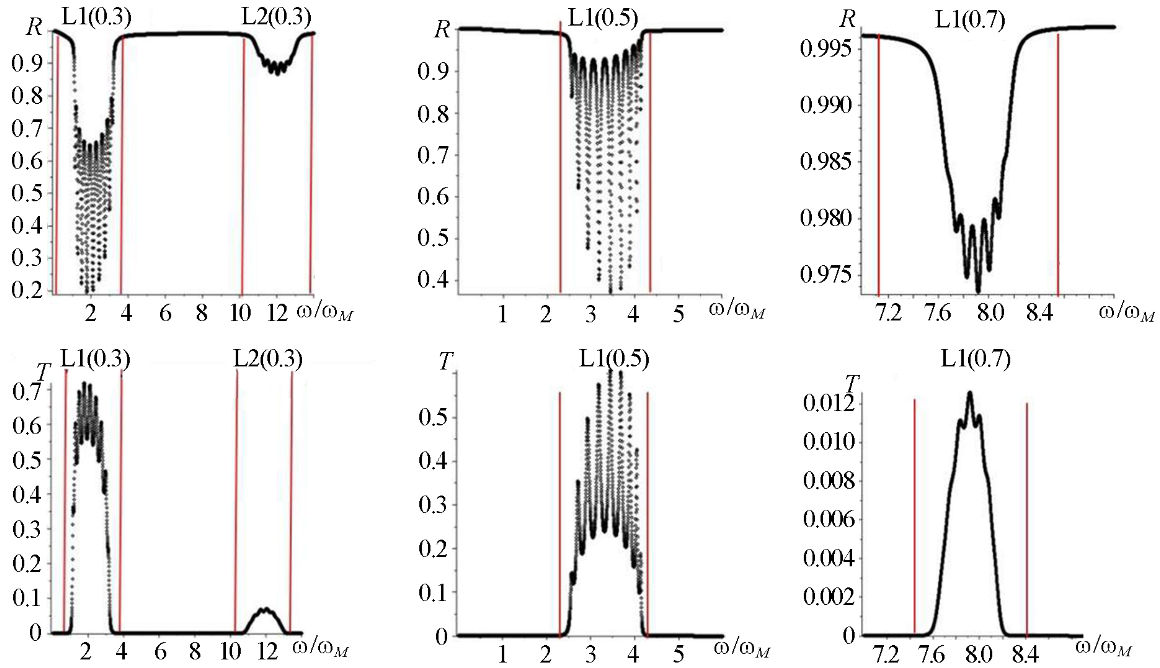

Fig. 6. Reflection coefficients (R) and transmission coefficients (T) for a wave of left polarization in a structure containing 10 antiferromagnetically ordered layers for values of relative thickness at Hilbert constants $\alpha_U = 0.01$, $\alpha_D = 0$. The vertical lines are the boundaries of the pass zones

Conclusion

The problems of propagation of waves of different nature in a periodic structure (or potential) have long been classical. However, a feature of spin waves is the presence of an additional degree of freedom associated with their polarization with respect to the equilibrium magnetization, which determines the nature of their propagation. Depending on it, the ESW are either running or evanescent. Therefore, by creating a symmetrical magnetic structure, it is possible to make the conditions for the propagation of waves of opposite polarization different, as can be seen from the ZT maps given in the work. We are talking about the difference in the propagation conditions of exchange waves, and not magnetodipole or exchange for dipole waves, since such non-reciprocity is also possible for them [18, 19].

Evanescent waves can also appear in problems of classical electrodynamics (waveguides). However, their appearance there is not associated with the presence of a dedicated direction and is determined either by the amount of energy relative to the potential at a given point, or as a characteristic feature of the equation itself (standing waves in the Laplace equation for a waveguide). The Kroning-Penny model can also be applied to this work, since the effective "potential"for the ESW arises due to the preservation of its polarization when crossing the boundaries of the cell interface.

References

1. Demokritov SO. Spin Wave Confinement: Propagating Waves. 2nd edition. Singapore: Pan Stanford Publishing; 2017. 448 p.
2. Poimanov VD, Kruglyak VV. Chirality of exchange spin waves exposed: Scattering and emission from interfaces between antiferromagnetically coupled ferromagnets. J. Appl. Phys. 2021;130(13):133902. DOI: 10.1063/5.0063727.

3. Poimanov VD, Shavrov VG, Kruglyak VV. Inhomogeneous converted spin waves in scattering problems. Journal of Radioelectronics. 2018;(11):7 (in Russian). DOI: 10.30898/1684-1719.2018.11.17.
4. Poimanov VD, Shavrov VG. Features of the scattering of exchange spin waves by layer and superlattice of biaxial ferromagnets. J. Phys. Conf. Ser. 2019;1389:012134. DOI: 10.1088/1742-6596/1389/1/012134.
5. Whitehead NJ, Horsley SAR, Philbin TG, Kuchko AN, Kruglyak VV. Theory of linear spin wave emission from a Bloch domain wall. Phys. Rev. B. 2017;96(6):064415. DOI: 10.1103/PhysRevB.96.064415.
6. Yan ZR, Xing YW, Han XF. Magnonic skin effect and magnon valve effect in an antiferromagnetically coupled heterojunction. Phys. Rev. B. 2021;104(2):L020413. DOI: 10.1103/PhysRevB.104.L020413.
7. Xing YW, Yan ZR, Han XF. Comparison of spin-wave transmission in parallel and antiparallel magnetic configurations. Phys. Rev. B. 2022;105(6):064427. DOI: 10.1103/PhysRevB.105.0644
8. Salanskii NM, Yerukhimov MS. Physical Properties and Applications of Thin Magnetic Films. Novosibirsk: Nauka; 1975. 222 p. (in Russian).
9. Goedsche F. Reflection and refraction of spin waves. Physica Status Solidi (B). 1970;39(1): K29–K33. DOI: 10.1002/pssb.19700390143.
10. Gorobets YI, Reshetnyak SA. Reflection and refraction of spin waves in uniaxial magnets in the geometrical-optics approximation. Tech. Phys. 1998;43(2):188–191. DOI: 10.1134/1.1258965.
11. Bass FG, Bulgakov AA, Tetervov AP. High-Frequency Properties of Semiconductors With Superlattices. Moscow: Nauka; 1989. 288 p. (in Russian).
12. Kruglyak VV, Kuchko AN. Spectrum of spin waves propagating in a periodic magnetic structure. Physica B: Condensed Matter. 2003;339(2–3):130–133. DOI: 10.1016/j.physb.2003.08.124.
13. Kruglyak VV, Davies CS, Tkachenko VS, Gorobets OY, Gorobets YI, Kuchko AN. Formation of the band spectrum of spin waves in 1D magnonic crystals with different types of interfacial boundary conditions. Journal of Physics D: Applied Physics. 2017;50(9):094003. DOI: 10.1088/1361-6463/aa536c.
14. Kruglyak VV, Kuchko AN. Effect of the modulation of magnetic viscosity on the damping of spin waves in multilayer magnetic systems. Phys. Metals Metallogr. 2001;92(3):211–214.
15. Kruglyak VV, Kuchko AN. Damping of spin waves in a real magnonic crystal. J. Magn. Magn. Mater. 2004;272–276(1):302–303. DOI: 10.1016/j.jmmm.2003.12.1246.
16. Latcham OS, Gusieva YI, Shytov AV, Gorobets OY, Kruglyak VV. Hybrid magnetoacoustic metamaterials for ultrasound control. Appl. Phys. Lett. 2020;117(10):102402. DOI: 10.1063/5.0018801.
17. Vysotskii S, Dudko G, Sakharov V, Khivintsev Y, Filimonov Y, Novitskii N, Stognij A, Nikitov S. Propagation of spin waves in ferrite films with metasurface. ACTA PHYSICA POLONICA A. 2018;133(3):508–510. DOI: 10.12693/aphyspola.133.508.
18. Vashkovskii AV, Stalmakhov VS, Sharaevskii YP. Magnetostatic Waves in Microwave Electronics. Saratov: Saratov University Publishing; 1993. 312 p. (in Russian).
19. Poimanov VD, Kruglyak VV. Nonreciprocity of propagation of exchange-dipole spin waves in two-layer magnetic films with crossed magnetization of the layers. J. Exp. Theor. Phys. 2022;134(5):615–629. DOI: 10.1134/s1063776122050107.